JOURNAL OF IRON AND STEEL RESEARCH, INTERNATIONAL. 2011, 18(12): 71-78

Workability Studies in Forming of Sintered Fe-0.35C Powder Metallurgy Preform During Cold Upsetting

S Narayan, A Rajeshkannan
[School of Engineering and Physics, Faculty of Science, Technology and Environment, University of the South Pacific (Laucala Campus), Suva, Fiji]

Abstract: An experimental investigation on the workability behaviour of sintered Fe-0.35C steel preforms under cold upsetting, have been studied in order to understand the influence of aspect ratio and lubrication condition on the workability process. The above mentioned powder metallurgy sintered preform with constant initial theoretical density of 84% of different aspect ratios, namely, 0.4 and 0.6 respectively were prepared using a suitable die-set assembly on a 1 MN capacity hydraulic press and sintered for 90 min at 1 200 ℃. Each sintered preform was cold upset under nil/no and graphite frictional constraint, respectively. Under the condition of triaxial stress densification state, axial stress, hoop stress, hydrostatic stress, effective stress and formability stress index against axial strain relationship was established and presented in this work. Further more, attained density was considered to establish formability stress index and various stress ratio parameters behaviour.

Key words: powder metallurgy; failure analysis; plastic behaviour; workability

Symbol List

D_0——Initial diameter of perform;
D_b——Forged bulged diameter of preform;
D_c——Forged contact diameter of preform;
f——Load;
h_0——Initial height of preform;
h_f——Forged height of preform;
R——Relative density;
R_0——Initial relative density;
S——Contact surface area;
ε_θ——True hoop strain;
ε_z——True axial strain;
σ_z——Axial stress;
σ_θ——Hoop stress;
σ_r——Radial stress;
σ_{eff}——Effective stress.

Powder metallurgy (P/M) parts have been widely applied in industry, particularly in aerospace and automobile industry[1] mainly because of their technical and economical advantages and provide reasons for researchers to analyze powder metallurgy materials behaviour under metal forming processes and the endeavor of the present researchers is to produce parts near the theoretical density; however, 100% dense component cannot be produced[2]. P/M technology produces net shape or near net shape components of extremely complex geometry and components of high strength and this technology is conducive nearly any material that can be processed in powder form[3]. Some fascinating parts can be made by beginning with a powder rather than a rod or billet. This process is one of the very few ways to create parts with controlled porosity. Such parts are of value in filtration applications for air and water. Alternatively, parts can be formed with high porosity and then the pores filled with other substances such as metals or lubricants. Powder based parts can be formed from material combinations virtually impossible with any other process[4]. Preforms are prepared in various steps that involve powder mixing, compacting and sintering known as primary deformation processes. A known limitation of this route is the residual porosity left in preforms after sintering process. A secondary deformation process such as

Biography: S Narayan(1980—), Male, Assistant Lecturer; **E-mail**: narayan_su@usp.ac.fj; **Received Date**: October 8, 2010

pressing or repressing, powder extrusion, powder rolling, and infiltration is used in order to enhance the mechanical properties of sintered powder materials[5]. The workability or formability of the P/M material plays a major role in determining if the P/M material will be formed successfully or fracture initiates in the forming process. Workability is a measure of the extent of deformation that a material can withstand induced internal stresses of forming prior to fracture occurred and is not only dependent on the ductility of the material but also on several forming parameters such as stress and strain rate, friction, temperature, etc[6-8].

Several constitutive equations have been proposed and studied to understand the constitutive behaviour of materials during forming operations[9-12] and later Abdel-Rahman and El-Sheikh M N[7], investigating the effect of relative density on the forming limit of P/M materials during upsetting also have proposed the stress formability criteria (β) for describing the effect of mean stress and the effective stress by employing theories proposed by Kuhn-Downey[13] and Whang-Kobayashi[4]. After conducting experiments on P/M compacts of several geometries it has been reported[14] that the initiation of the ductile fracture can be predicted. The attention on the hoop stress, hydrostatic stress and axial stress behaviour of any P/M materials is much required for any cold forging process and Narayanamurti et al[15] presented some of the important criteria generally used for the prediction of ductile fracture. Deformation control to avoid fracture can be established by careful selection of process parameters, the factors being die shaping, lubrication, preform shape, preform dimensions and density. Geometrical design of the preform in metal forging of complex parts has great effects on the forging load and plays a key role in improving product quality, such as ensuring defect-free product and proper metal flow. The formability limit of powder metallurgy material is usually determined by visible crack initiation on the free surface. By careful selection of process parameter and deformation process, densification can be enhanced and crack appearance on the deforming preforms can be avoided by increasing the compressive level of stresses on the material[16-18]. Lubrication also influences metal flow in a generally beneficial manner with respect to crack formation. Lubrication is important in most metal forming processes particularly in cold metal forming because good lubrication improves the quality of products through the reduction of defects and improvement in the dimensional accuracy and surface finish[19-21]. Thus, the present investigation is aimed to establish the workability limit under triaxial stress state condition of powder metallurgy preforms of Fe-0.35C experimentally under two different frictional constraints, namely, nil/no lubricant condition and graphite lubricant condition and of two different aspect ratios of 0.4 and 0.6, respectively, and to establish the technical relationship that exists between the characteristics of axial stress, hoop stress, hydrostatic stress, effective stress and formability stress index with respect to true height strain and densification. Furtherly, the technical relationship was established that exists between stress ratio parameters, namely, $(\sigma_\theta/\sigma_{eff})$, (σ_m/σ_{eff}) and (σ_z/σ_{eff}) with respect to percent fractional theoretical density and axial strain.

1 Experimental Details

1.1 Materials and characterization

Atomized iron powder of less than or equal to 150 μm size and graphite powder of 2 to 3 μm size were used in the present investigation. Analysis indicated that the purity of iron was 99.7% and the rest were insoluble impurities. The characteristics (apparent density, flow rate and particle size distribution) of iron powder and Fe-0.35C blends are shown in Table 1 and Table 2.

Table 1 Characterization of iron powder

Si No.	Property	Iron	Fe-0.35C Blend
1	Apparent density/(g · mL^{-1})	3.38	3.37
2	Flow rate (s/50g) by Hall Flow Meter	26.3	28.1
3	Compressibility at pressure of 430±10 MPa (g · mL^{-1})	6.46	6.26

Table 2 Sieve size analysis of iron powder

Sieve size/μm	150	+125	+100	+75	+63	+45	−45
Mass percent (Ret.)	10.60	24.54	15.46	19.90	11.10	8.40	10.00

1. 2 Blending, compaction and sintering

A powder mix corresponding to Fe-0. 35C was taken in a stainless steel pot with the powder mixed to porcelain balls (10—15 mm diameter) with a ratio of 1 : 1 by mass. The pot containing the blended powder was subjected to the blending operation by securely tightening and then fixing it to the pot mill. The mill was operated for 20 h to obtain a homogenous mix. Green compacts of 28 mm diameter with 18 mm of length were prepared. The powder blend was compacted on a 1. 0 MN hydraulic press using a suitable die, a punch and a bottom insert in the pressure range of 430±10 MPa to obtain an initial theoretical density of 0. 84±0. 01. In order to avoid oxidation during sintering and cooling, the entire surface of the compacts were indigenously formed ceramic coated. These ceramic coated compacts were heated in the controlled atmosphere furnace with argon gas purging (at 15 L/min) at a temperature of 1200 ℃±10 ℃. At this temperature the compacts were sintered for 90 min followed by furnace cooling.

1. 3 Cold deformation

Sintered and furnace cooled preforms were machined to such a dimension so as to provide height-to-diameter ratio of 0. 40 (24 mm in diameter with 10 mm in height) and 0. 60 (26 mm in diameter with 16 mm in height), respectively. The initial dimensions of the cylindrical preforms were measured and recorded and used to calculate the initial density. Each specimen was compressively deformed between a flat die-set in the incremental loading step of 0. 05 MN using 1 MN capacity hydraulic press under friction conditions, which included dry, unlubricated dies called nil/no lubricant condition and lubrication consisting of graphite paste (i. e. graphite with acetone) called graphite lubricant condition. The deformation process was stopped once a visible crack appeared at the free surface. Dimensional measurements such as deformed height, deformed diameters (including bulged and contact) were carried out after every step of deformation using digital vernier caliper and the density measurements being carried out using the Archimedes principle. Experimental results were used to calculate the axial stress, hoop stress, hydrostatic stress, effective stress, various stress ratio parameters, namely, $(\sigma_\theta/\sigma_{\text{eff}})$, $(\sigma_m/\sigma_{\text{eff}})$ and $(\sigma_z/\sigma_{\text{eff}})$, true height strain, percentage theoretical density and formability stress index.

2 Theoretical Analysis

Using the measured upsetting parameters the following mathematical expressions are used to determine other upsetting parameters (axial stress, hoop stress, hydrostatic stress, effective stress and axial strain) for triaxial stress state. The expression for true axial stress for powder metallurgy materials is as follows:

$$\sigma_z=\frac{f}{S} \tag{1}$$

According to Abdel-Rahman and M N El-Sheikh[7], the expression for the axial strain (ε_z) can be written as follows:

$$\varepsilon_z=\ln\left[\frac{h_0}{h_f}\right] \tag{2}$$

And true hoop strain is

$$\varepsilon_\theta=\ln\left[\frac{2D_b^2+D_c^2}{3D_0^2}\right] \tag{3}$$

The plastic deformation behaviour of porous metals is influenced by the internal pores and the analysis of porous metals requires an appropriate yield criterion which should take the pore effect into account. Many researchers over the years have analyzed several different yield criteria for sintered powder materials which are based on experimental and theoretical analysis[9,22-23]. A typical theorem is that the plastic deformation occurs when the elasticity strain energy reaches a critical value. The formulation can be written as

$$AJ_2^1+BJ_1^2=Y^2=\delta Y_0^2 \tag{4}$$

where A, B, δ are yield criterion parameters and are functions of relative density, J_1 is the first invariant of the stress tensor, J_2^1 is the second invariant of the stress deviator and Y_0 and Y are yield strength of a solid and partially dense material having relative density R, respectively[23]. The parameters J_1 and J_2^1 in the cylindrical coordinate system where the axis represents radial, circular and axial direction can be expressed as follows

$$J_2^1=\frac{1}{6}[(\sigma_r-\sigma_\theta)^2+(\sigma_\theta-\sigma_z)^2+(\sigma_z-\sigma_r)^2] \tag{5}$$

and

$$J_1=\sigma_r+\sigma_\theta+\sigma_z \tag{6}$$

Here for axisymmetric forging, $\sigma_r=\sigma_\theta$, J_2^1 and J_1^2 can be written as

$$J_2^1=\frac{1}{6}(2\sigma_\theta^2+2\sigma_z^2-4\sigma_\theta\sigma_z) \tag{7}$$

and

$$J_1^2=4\sigma_\theta^2+\sigma_z^2+4\sigma_\theta\sigma_z \tag{8}$$

Substituting Eqn. (7) and Eqn. (8) into Eqn. (4) gives

$$\frac{A}{6}(2\sigma_\theta^2+2\sigma_z^2-4\sigma_\theta\sigma_z)+B(4\sigma_\theta^2+\sigma_z^2+4\sigma_\theta\sigma_z)=\delta Y_0^2 \tag{9}$$

L Hua et al[9] has investigated and presented the values for yield criterion parameters based on plastic Poisson's ratio, relative density and flow stress of the matrix material and several yield criterions for sintered powder material were also compared with each other. The following yield criteria parameters are chosen in this research as $A=2+R^2$, $B=(1-R^2)/3$, $\delta=[(R-R_0)/(1-R_0)]^2$. Eqn. (9) now can be written as

$$Y_0=\sigma_{\text{eff}}=\left\{\frac{(1-R_0)^2[\sigma_z^2-2\sigma_\theta^2-R(\sigma_\theta^2-2\sigma_\theta\sigma_z)]}{(R-R_0)^2}\right\}^{0.5} \tag{10}$$

Eqn. (10) gives the expression for effective stress in terms of cylindrical coordinates.

According to R Narayansamy et al[6], the state of stress in a triaxial stress condition is given by

$$\alpha=\frac{(2+R^2)\sigma_\theta-R^2(\sigma_z+2\sigma_\theta)}{(2+R^2)\sigma_z-R^2(\sigma_z+2\sigma_\theta)} \tag{11}$$

Using Eqn. (11) for the values of Poisson's ratio (α), relative density (R) and axial stress (σ_z), the hoop stress (σ_θ) under triaxial stress state condition can be determined as given below:

$$\sigma_\theta=\left[\frac{2\alpha+R^2}{2-R^2+2R^2\alpha}\right]\sigma_z \tag{12}$$

where, $\alpha=\frac{d\varepsilon_\theta}{d\varepsilon_z}$.

The stress formability factor[7] is given as

$$\beta=\frac{J_1}{(3J_2^1)^{0.5}}=\frac{3\sigma_m}{\sigma_{\text{eff}}} \tag{13}$$

where, $\sigma_m=\frac{\sigma_r+\sigma_\theta+\sigma_z}{3}=\frac{2\sigma_\theta+\sigma_z}{3}$, is the hydrostatic stress.

The stress formability factor as expressed in Eqn. (13) is used to describe the effect of mean stress and the effective stress on the forming limit of P/M compacts in upsetting.

3 Results and Discussion

Fig. 1 shows the relationship between fractional theoretical density and true height strain for Fe-0.35C P/M preform cold deformed under two different frictional conditions, namely, nil/no and graphite lubricant conditions. It is noted that the densification is higher during the initial stages of deformation with reduced height strain followed by steady state response

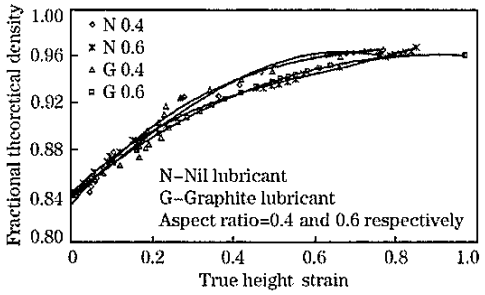

Fig. 1 Variation of fractional theoretical density against true height strain for cold deformed Fe-0.35C preform

and at the final stage of deformation very little increase in densification is achieved indicating the P/M preform has strain hardened. The presence of larger pores during the initial stages of deformation promotes densification significantly with little enhancement in axial strain, however, as the deformation progresses the pore closing rate decreases reducing the densification rate during the intermediate stage. Furtherly, it is found that 0.40 aspect ratio preform densification values are improved for any true height strain value when compared to the 0.6 aspect ratio preform provided the preforms initial theoretical density are same, however, the final densification achieved before crack initiation on the free surface of the preforms is marginally different. Also, it can be seen that the true height strain at fracture is higher in the case of graphite employed lubricant for 0.6 aspect ratio preform, however, in the case of 0.4 aspect ratio preform the strain at fracture is marginally different for the two lubricants used.

It has been reported[7] that the effect of relative density is a major concern on formability of P/M material. It is imperative to note that the extent to which P/M material are formed as well as maximum density been achieved are the major concerns for structural applications. Therefore Fig. 2 and Fig. 3 show the relationship between formability stress index against true height strain and fractional theoretical density, respectively, for Fe-0.35C P/M preform cold deformed under two different frictional conditions, namely, nil/no and graphite lubricant conditions. From Fig. 2, it is noted that for any given true height strain the formability stress index is the highest for lower aspect ratio preform deformed under nil/no lubricant condition. The final formability stress index value achieved is almost the same, however, at different fracture strain values. Furtherly, from Fig. 3, it is noted that the effect of aspect ratio and

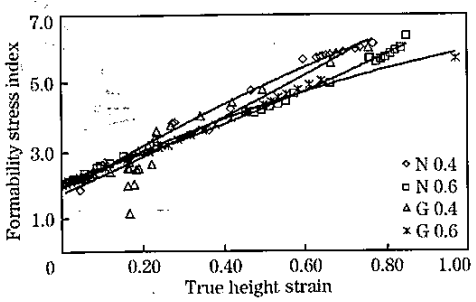

Fig. 2 Variation of formability stress index against true height strain for cold deformed Fe-0. 35C preform

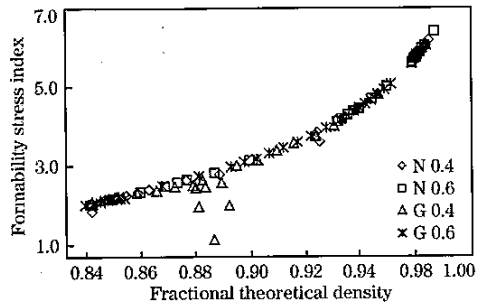

Fig. 3 Variation of formability stress index against fractional theoretical density for cold deformed Fe-0. 35C preform

frictional constraints on the formability stress index plotted against fractional theoretical density is literally nil. As the density approaches near theoretical density the formability stress index value increases sharply.

Fig. 4 shows the relationship between axial stress and true height strain for Fe-0. 35C P/M preform cold deformed under two different frictional conditions, namely, nil/no and graphite lubricant conditions. The axial stress increases rapidly during the initial stages of deformation with little enhancement in true height strain as the initial application of load is not enough to effectively close the pores but only increases the internal energy of the particles. The axial stress value is the highest in the lower aspect ratio preform deformed under nil/no lubricant condition for any given true height strain value. The lateral deformation is more pronounced in the graphite employed preform. From Fig. 5 it can be seen that the pores (black color) are more elongated for graphite employed lubricant when compared to nil/no lubricant condition and from Fig. 1 it can be seen that densification is pronounced in the case of lower aspect ratio, these being the reasons for enhanced axial stress values for lower aspect ratio preform deformed under nil/no lubricant condition.

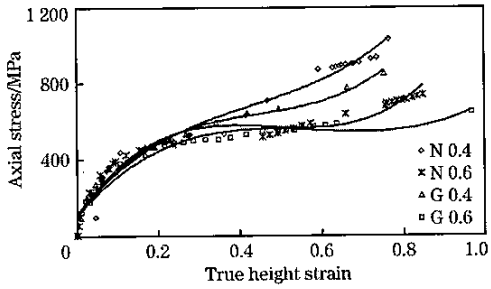

Fig. 4 Variation of axial stress against true height strain for cold deformed Fe-0. 35C preform

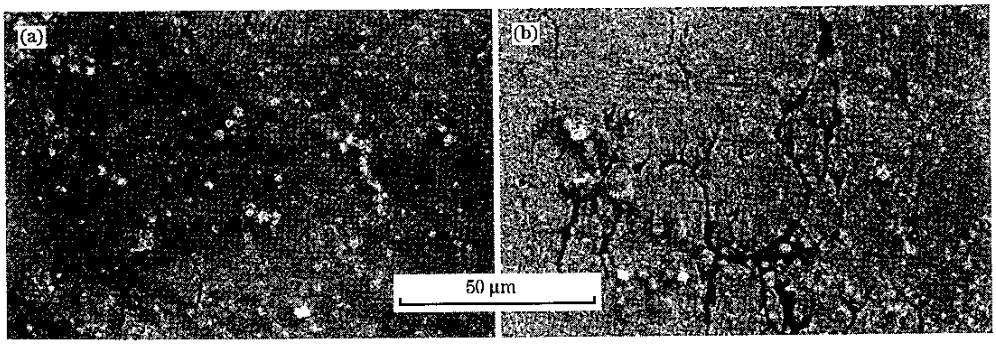

Fig. 5 Microstructure view at diametric extreme of preform deformed under nil/no and graphite employed lubricant respectively

Fig. 6 and Fig. 7 show the relationship between axial, hydrostatic, hoop and effective stresses against true height strain for Fe-0. 35C P/M preform cold deformed under nil/no lubricant condition and graphite lubricant condition, respectively. From Fig. 6 it is clearly seen that the difference between hoop stress, hydrostatic stress and axial stress is literally nil for preform deformed under nil/no lubricant condition but for preform deformed under graphite lubricant condition (Fig. 7) the difference between the aforementioned stresses are prominent, however, the difference is only evident during initial stages of de-

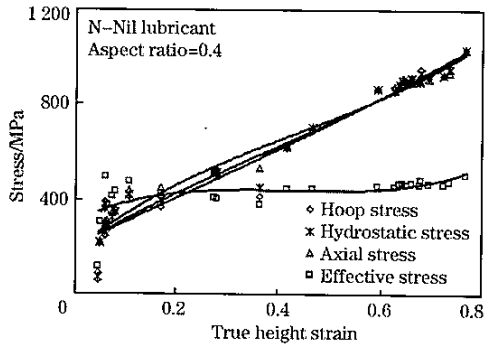

Fig. 6 Variation of hydrostatic, hoop, axial and effective stresses against true height strain for Fe-0. 35C P/M preform deformed under nil lubricant condition

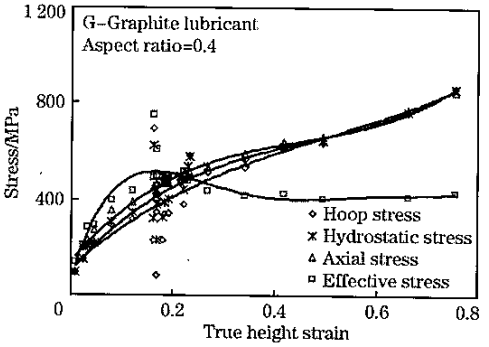

Fig. 7 Variation of hydrostatic, hoop axial and effective stresses against true height strain for Fe-0. 35C P/M preform deformed under graphite lubricant condition

formation. Hence, this difference in aforementioned stresses can be neglected for all practical purpose for Fe-0. 35C P/M preform. The behaviour of hydrostatic stress and hoop stress against true height strain is similar to that of axial stress against true height strain discussed earlier. Furtherly, it is noted that the effective stress is significantly lower than the aforementioned stresses irrespective of lubricant employed.

Fig. 8 shows the relationship between effective stress and true height strain for Fe-0. 35C P/M preform cold deformed under two different frictional conditions, namely, nil/no and graphite lubricant conditions. The characteristics nature of the curves is similar. The effective stress increases rapidly for low true height strain values followed by gradual decrease up to a height strain of approximately 0. 4 and therefater remains almost constant until fracture. For any given true height strain the effective stress is found to be the highest for lower aspect ratio preform deformed under nil/no lubricant condition as effective closure of pores (Fig. 5) occurs with higher

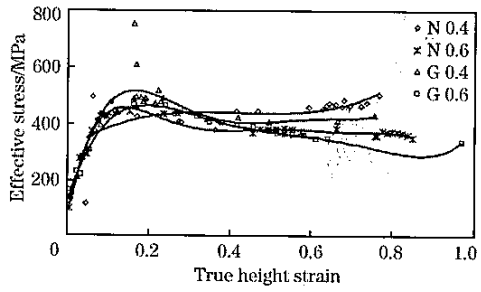

Fig. 8 Variation of effective stress against true height strain for cold deformed Fe-0. 35C preform

densification (Fig. 1) under these conditions.

Fig. 9 and Fig. 10 show the relationship between stress ratio parameter (σ_z/σ_{eff}) against relative density and true height strain, respectively, for Fe-0. 35C P/M preform cold deformed under two different frictional conditions, namely, nil/no and graphite lubricant conditions. The characteristics nature of the curves plotted are similar and as the densification and axial strain increases the stress ratio parameter, σ_z/σ_{eff}, also increases. As seen from Fig. 9 the effect of aspect ratio and lubricant conditions on the stress ratio parameter, σ_z/σ_{eff}, is literally nil, however, when plotted against axial strain (Fig. 10) the effect is prominent. The stress ratio parameter (σ_z/σ_{eff}) is found to be higher in lower aspect ratio preform in co-

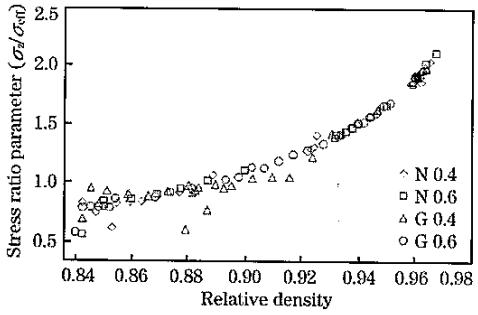

Fig. 9 Variation of stress ratio parameter (σ_z/σ_{eff}) against relative density for cold deformed Fe-0. 35C preform

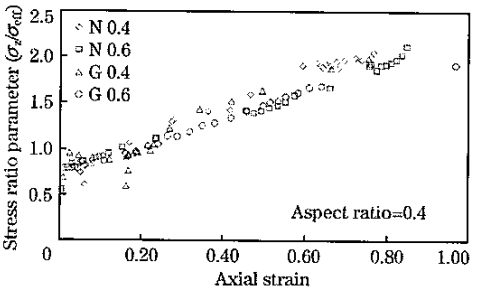

Fig. 10 Variation of stress ratio parameter (σ_z/σ_{eff}) against axial strain for cold deformed Fe-0. 35C preform

mparison to higher aspect ratio preform for any given axial strain irrespective of lubricant conditions (Fig. 10). This is due to the fact that the pore closure mechanism is faster in lower aspect ratio preform due to the lower pore bed height in comparison with higher aspect ratio preform and hence densification increases for lower aspect ratio preform (Fig. 1) which in turn increases the stress and stress ratio parameter for lower aspect ratio preform.

Fig. 11 and Fig. 12 show the relationship between stress ratio parameters ($\sigma_\theta/\sigma_{eff}$), ($\sigma_m/\sigma_{eff}$) and ($\sigma_z/\sigma_{eff}$) against relative density and axial strain for Fe-0. 35C P/M preform cold deformed under nil/no lubricant condition and graphite lubricant condition, respectively. It is seen that the difference between the above mentioned stress ratio parameters plotted against relative density (Fig. 11) and axial strain (Fig. 12) is literally nil, and hence, the behaviour of above mentioned stress ratio parameters against relative density and axial strain is similar to that of discussed earlier between σ_z/σ_{eff} against relative density (Fig. 9) and σ_z/σ_{eff} against axial strain (Fig. 10), respectively.

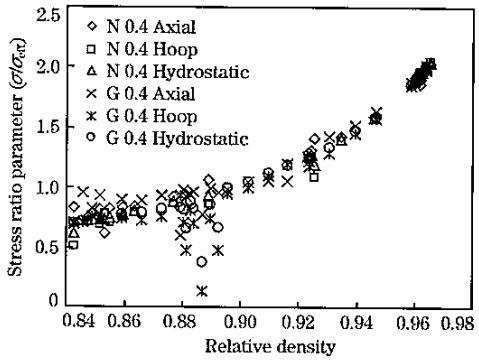

Fig. 11 Variation of stress ratio parameters ($\sigma_\theta/\sigma_{eff}$), ($\sigma_m/\sigma_{eff}$) and ($\sigma_z/\sigma_{eff}$) against relative density

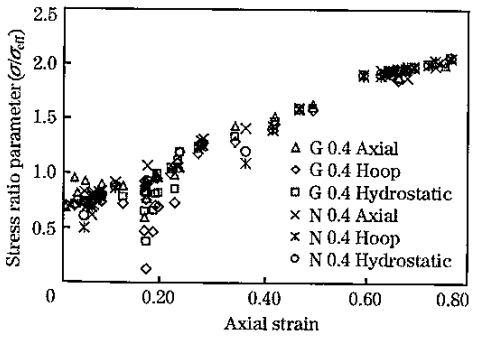

Fig. 12 Variation of stress ratio parameters ($\sigma_\theta/\sigma_{eff}$), ($\sigma_m/\sigma_{eff}$) and ($\sigma_z/\sigma_{eff}$) against axial strain

4 Conclusions

1) The amount of densification and formability stress index is found to be high when decreasing aspect ratio and increasing friction conditions, however, the final achievements of densification and formability stress index are almost the same irrespective of the variables used in the investigation. Furthermore, it is evident that other workability parameters like axial stress, hoop stress, hydrostatic stress, effective stress and various stress ratio parameters are enhanced with the decreasing aspect ratio and increasing friction conditions.

2) The difference observed between axial stress, hydrostatic stress and hoop stress against axial strain and promoted densification is literally nil irrespective of the frictional conditions and preform geometry. Also, the effect of stress ratio parameters ($\sigma_\theta/\sigma_{eff}$, σ_m/σ_{eff} and σ_z/σ_{eff}) against induced strain and promoted densification is practically negligible for all the concerned preforms.

References:

[1] Lindskog P. Economy in Car-Making—Powder Metallurgy [R]. London: Global Automotive Manufacturing and Technology, Business Briefing, 2003.

[2] Mamalis A G, Petrossian G L, Manolakos D E. Limit Design of Porous Sintered Metal Powder Machine Elements [J]. J Mater Process Technol, 2000, 98: 335.

[3] Zhang X Q, Peng Y H, Li M Q, et al. Study of Workability Limits of Porous Materials Under Different Upsetting Conditions by Compressible Rigid Plastic Finite Element Method [J]. J Mater Eng Perform, 2000, 9: 164.

[4] Rosochowski A, Beltrando L, Navarro S. Modeling of Density and Dimensional Changes in Re-Pressing/Sizing of Sintered Components [J]. J Mater Process Technol, 1998, 80: 188.

[5] Kandavel T K, Chandramouli R, Ravichandran M. Experimental Study on the Plastic Deformation and Densification Characteristics of Some Sintered and Heat Treated Low Alloy Powder Metallurgy Steels [J]. Mater Des, 2010, 31: 485.

[6] Narayanasamy R, Ramesh T, Pandey K S. Some Aspects on Workability of Aluminium-Iron Powder Metallurgy Composite During Cold Upsetting [J]. Mater Sci Eng, 2005, 391: 418.

[7] Rahman M A, El-Sheikh M N. Workability in Forging of Powder Metallurgy Compacts [J]. J Mater Process Technol, 1995, 54: 97.

[8] El-Domiatry A, Shaker M. A Note on the Workability of Porous-Steel Preforms [J]. J Mater Process Technol, 1991, 25: 229.

[9] Qin X P, Hua L. Deformation and Strengthening of Sintered Ferrous Material [J]. J Mater Process Technol, 2007, 188: 694.

[10] Kuhn H A, Lawley A. Powder Metallurgy Processing [M]. 1st ed. New York: Academic Press, 1978.

[11] Taha M A, El-Mahallawy N A, El-Sabbagh A M. Some Experimental Data on Workability of Aluminium-Particulate-Reinforced Metal Matrix Composites [J]. J Mater Process Technol, 2008, 202: 380.

[12] Doraivelu S M, Gegel H L, Gunasekera J, et al. New Yield Function for Compressible P/M Materials [J]. Int J Mech Sci, 1984, 26: 527.

[13] Kuhn H A, Downey C L. How Flow and Fracture Affect Design of Preforms for Powder Forging [J]. Int J Powder Metall Powder Technol, 1974, 10: 59.

[14] Gouveia B P P A, Rodrigues J M C, Martins P A F. Ductile Fracture in Metalworking: Experimental and Theoretical Research [J]. J Mater Process Technol, 2000, 101: 52.

[15] Narayanamurti S V S, Nageswara B R, Kashyap B P. Improved Ductile Fracture Criterion for Cold Forming of Spheroidised Steel [J]. J Mater Process Technol, 2004, 147: 94.

[16] Butuc M C, Gracio J J, Rocha B A. An Experimental and Theoretical Analysis on the Application of Stress-Based Forming Limit Criterion [J] Int J Mech Sci, 2006, 48: 414.

[17] Lee S R, Lee Y K, Park C H, et al. A New Method of Preform Design in Hot Forging by Using Electric Field Theory [J]. Int J Mech Sci, 2002, 44: 773.

[18] Sedighi M, Tokmechi S. A New Approach to Preform Design in Forging Process of Complex Parts [J]. J Mater Process Technol, 2008, 197: 314.

[19] Rajeshkannan A, Narayan S. Strain Hardening Behaviour in Sintered Fe-0.8%C-1.0%Si-0.8%Cu Powder Metallurgy Preform During Cold Upsetting [J]. J Eng Manufacture, 2009, 223: 1567.

[20] Ramesh B, Senthivelan T. Formability Characteristics of Aluminium Based Composite-A Review [J]. Int J Eng Technol, 2010, 2: 1.

[21] Simchi A. Effects of Lubrication Procedure on the Consolidation, Sintering and Microstructural Features of Powder Compacts [J]. Mater Des, 2003, 24: 585.

[22] Han H N, Oh K H, Lee D N. Analysis of Forging Limit for Sintered Porous Metals [J]. Scripta Metallurgica et Materialia, 1995, 32: 1937.

[23] Lewis R W, Khoei A R. A Plasticity Model for Metal Powder Forming Processes [J]. Int J Plast, 2001, 17: 1659.